Applied Physics Letters

Radiative and Auger recombination processes in indium nitride

Cite as: Appl. Phys. Lett. **112**, 251108 (2018); https://doi.org/10.1063/1.5038106
Submitted: 01 May 2018 . Accepted: 07 June 2018 . Published Online: 20 June 2018

Andrew McAllister, Dylan Bayerl, and Emmanouil Kioupakis

Radiative and Auger recombination processes in indium nitride

Andrew McAllister,[1] Dylan Bayerl,[2] and Emmanouil Kioupakis[2,a)]
[1]*Applied Physics Program, University of Michigan, Ann Arbor, Michigan 48109, USA*
[2]*Materials Science and Engineering, University of Michigan, Ann Arbor, Michigan 48109, USA*

(Received 1 May 2018; accepted 7 June 2018; published online 20 June 2018)

InN and In-rich InGaN alloys emit in the infrared range desirable for telecommunication applications. However, the droop problem reduces their efficiency at high power. Nonradiative Auger recombination is a strong contributor to this efficiency loss. Here, we investigate radiative and Auger recombination in InN and In-rich InGaN with first-principles calculations. We find that the direct eeh process dominates Auger recombination in these materials. In the degenerate carrier regime, the Auger and radiative rates are suppressed by different mechanisms: the radiative rate is affected by phase-space filling while Auger recombination is primarily reduced by free-carrier screening. The suppression of the radiative rate onsets at lower carrier densities than that of the Auger rate, which reduces the internal quantum efficiency of InN devices. Droop in InN can be mitigated by increasing the bandgap through alloying with GaN. We demonstrate that the peak efficiency of $In_{0.93}Ga_{0.07}N$ alloys (which emit at 1550 nm) is 33% higher than that of InN and occurs at higher carrier densities. *Published by AIP Publishing*. https://doi.org/10.1063/1.5038106

The group-III nitrides (AlN, GaN, and InN) and their alloys are leading materials for light-emitting diodes (LEDs) and lasers. Their direct bandgaps span 0.7–6.2 eV—ranging from the ultraviolet (UV) to the infrared (IR) ranges.[1] In-rich InGaN emits in the IR and could be used for telecommunications, where fast, secure, and efficient light emission and detection are necessary. Although other materials are used commercially for IR applications, ongoing efforts to develop IR nitride devices[2–4] focus on their tunability, resistance to radiation, low toxicity, and fast switching speeds.

While nitrides have many appealing optoelectronic properties, their devices suffer from the "efficiency droop" problem, i.e., the reduction of the internal quantum efficiency (IQE) at high current densities.[5] Both experimental[6] and theoretical[7] studies point to non-radiative Auger recombination as the primary cause of the efficiency droop. In Auger recombination, an electron and a hole recombine and give excess energy to another carrier instead of emitting a photon, which is the desired, radiative process [Fig. 1(a)]. The excited carrier can either be an electron [electron-electron-hole or *eeh* process, Fig. 1(b)] or a hole (hole-hole-electron or *hhe* process). In addition, Auger can be assisted by phonons, which enable the overall momentum conservation [Fig. 1(c)].

For non-degenerate carriers, the radiative rate is proportional to the square of the free-carrier density n, $R_{rad} = dn/dt = Bn^2$ (assuming equal free electron and hole densities, which applies to optical excitation experiments of undoped samples), while the Auger rate is proportional to the cube of the density, $R_{Auger} = Cn^3$, where B and C are the radiative and Auger recombination coefficients, respectively. Therefore, at high densities, the Auger process dominates and causes an efficiency loss in devices. The corresponding lifetimes [$\tau = n/(dn/dt)$] are $\tau_{rad} = 1/Bn$ and $\tau_{Auger} = 1/Cn^2$.

But for degenerate carrier concentrations, the radiative and Auger rates are reduced from the quadratic and cubic dependence on the density, respectively, an effect known as phase-space filling.[8] For nondegenerate carrier densities, the occupations of electron and hole states are approximated by Maxwell-Boltzmann statistics and are proportional to the carrier density. Therefore, the number of holes that can recombine with each electron is proportional to the total number of holes, and hence, the radiative lifetime is inversely proportional to the carrier density. However, for degenerate carriers, the occupations are described by Fermi-Dirac statistics and approach the limiting value of 1. In this limit, the number of holes that can recombine with each electron (and hence the radiative lifetime) are independent of the total hole concentration. Similar arguments apply to Auger recombination. Phase-space filling is detrimental for droop because it increases the steady-state carrier density for a given current density and thus increases the fraction of carriers that recombine via Auger.[9] For degenerate carriers, the radiative rate becomes $R_{rad} = B'n$ while the power law of the Auger rate becomes quadratic, $R_{Auger} = C'n^2$, where B' and C' are the degenerate radiative and Auger coefficients, respectively.[8] The corresponding lifetimes become $\tau_{rad} = 1/B'$ and $\tau_{Auger} = 1/C'n$.

The Auger rate is further reduced at high carrier densities due to screening by free carriers. Screening in this context

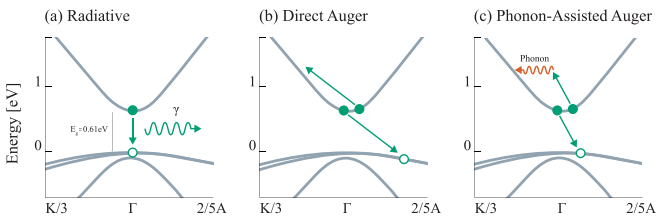

FIG. 1. The quasiparticle (G_0W_0) band structure of InN, along with schematics of (a) radiative and (b) and (c) Auger recombination. In the Auger process (b), an electron and a hole recombine and excite another carrier to a higher energy state. The indirect Auger process (c) is mediated by the emission or absorption of a phonon, which transfers momentum to the electrons and enables additional Auger transitions that are otherwise forbidden by energy and momentum conservation.

a)Electronic mail: kioup@umich.edu

does not refer to the screening of the polarization fields in polar LEDs but rather to the suppression of the Coulomb interactions between free carriers due to their mutual shielding. Moreover, the density-dependence of the recombination rates is unclear for intermediate carrier densities at which electrons are degenerate but holes are not, as is often the case for InN. To account for the changing power law of the recombination rates on the density, it is common in the literature to express the radiative and Auger coefficients as functions of the density, $B(n)$ and $C(n)$, respectively.[10] Moreover, the density dependence of both coefficients is often assumed to be the same, apart from a different prefactor.[10–13] Overall, a predictive understanding of the density dependence of radiative and Auger recombination for degenerate carriers in semiconductors is needed to design more efficient optoelectronic devices at high power.

Although the LED droop problem has motivated numerous studies of carrier recombination in Ga-rich InGaN, fewer studies have focused on the narrower-gap nitrides such as InN and In-rich InGaN. Tsai, Chang, and Gwo[14] used pump-probe, time-resolved reflectivity measurements to determine Auger rates in degenerate InN. Fitting these data yielded a degenerate Auger coefficient of $C' = 2.48 \times 10^{-10}\,\mathrm{cm^3\,s^{-1}}$ and an Auger lifetime of 400 ps. Jang *et al.*[15] used time-resolved photoluminescence to study Auger recombination in two degenerately doped InN samples at varying temperatures (35–300 K). The Auger coefficients for the two samples differed by one order of magnitude ($10^{-29}\,\mathrm{cm^6\,s^{-1}}$–$10^{-30}\,\mathrm{cm^6\,s^{-1}}$ or lifetimes from 230 to 1200 ps) at 300 K. They observed a weak temperature dependence and n^2 density dependence of the Auger rate and attributed this to Auger being mediated by phonons rather than an effect from phase-space filling. Cho *et al.*[16] studied Auger recombination of degenerately doped InN using photoluminescence at room temperature. They fitted the Auger coefficient and its density dependence to the spectra and found a degenerate Auger coefficient of $4.5 \pm 2 \times 10^{-9}\,\mathrm{cm^3\,s^{-1}}$ corresponding to a lifetime of 20 ps. Finally, Chen *et al.*[17] studied three samples of InN at 20 K and 300 K using time-resolved pump-probe transmission measurements and observed carrier lifetimes inversely proportional to the density. Although this density dependence is consistent with degenerate Auger recombination, the authors attribute the lifetimes entirely to radiative and defect recombination and rule out the possibility of Auger. Auger recombination in InGaN alloys was also studied with first-principles calculations by Delaney *et al.*[18] They found that in the In-rich limit, Auger recombination occurs via intraband processes, with a coefficient of $\sim 4 \times 10^{-30}\,\mathrm{cm^6\,s^{-1}}$. However, their InGaN calculations for band structures and wave functions were performed for GaN and extrapolated to different alloy compositions by shifting the bandgap, which is not optimal for In-rich alloys.

In this work, we performed first-principles calculations to understand the radiative and Auger recombination properties of bulk indium nitride as a function of free-carrier density. We found that the dominant Auger mechanism is the direct *eeh* process. We also uncovered that for degenerate carriers, screening between carriers is the primary mechanism of reducing the Auger rate power law, rather than phase-space filling. We further found that the radiative rate is suppressed by phase-space filling at lower carrier densities than the Auger rate is suppressed by screening or phase-space filling, which is detrimental to the efficiency of devices. Finally, alloying InN with GaN to increase the bandgap reduces the Auger rate and increases the internal quantum efficiency.

Our calculations are based on density functional (DFT) and many-body perturbation theory. We performed plane-wave norm-conserving pseudopotential DFT calculations with the local density approximation (LDA)[20] for the exchange-correlation functional and the Quantum Espresso[19] code. The relaxed lattice parameters of InN are $a = 6.69$ and $c = 10.83$ Bohr. For the band structure, we included a Hubbard U correction (LDA + U) for the In $4d$ and the N $2p$ orbitals to avoid the artificial closing of the gap of InN by LDA and the subsequent unphysical mixing of valence and conduction states near Γ. Our U parameters ($U_p = 1.5\,\mathrm{eV}$ and $U_d = 6.0\,\mathrm{eV}$) were obtained from Ref. 21. Even with the U correction, LDA does not correctly predict the bandgap of InN, which is needed for recombination rate calculations. We therefore perform G_0W_0 calculations[22] with the BerkeleyGW code[23] to correct the LDA + U eigenvalues.

The G_0W_0 band structure near the band edges is shown in Fig. 1. Our calculated G_0W_0 bandgap of InN is 0.61 eV, which agrees with the experimental range of measurements (0.6–0.8 eV)[16,24–27] that depend on doping and temperature. To account for these sample-dependent gap variations on the recombination rates, we rigidly varied the bandgap over the 0.5–0.8 eV range. This adjustment of the gap value further allows us to assess the convergence of out rate calculations and to simulate the effect of alloying with GaN. Our calculated electron effective mass ($0.07\,m_e$) also agrees with experiment.[28] To obtain radiative and Auger coefficients, we used the maximally localized Wannier function method[29] and the wannier90 code[30] to interpolate the band energies and velocity matrix elements onto fine Brillouin-zone (BZ) grids. The rates were calculated using Fermi's Golden Rule[31] and the methodology of Refs. 9 and 32. We used a $100 \times 100 \times 50$ grid for the *eeh* and an $80 \times 80 \times 40$ grid for the *hhe* process. Gaussian functions with a width of 0.1 eV are used to evaluate the energy delta functions in the Auger rates. The screened Coulomb matrix elements were evaluated using the model dielectric function of Cappellini *et al.*[33] and the experimental high frequency dielectric constant of InN ($\epsilon_\infty = 8.4$).[34] The lattice and electronic temperatures are set to 300 K.

We begin by identifying the dominant Auger process in InN. The small bandgap of the material suggests that direct Auger is most important, in agreement with the universal trends for semiconductors discussed by Bulashevich and Karpov.[35] Intuitively, additional scattering from phonons is not needed to conserve momentum during the Auger process in InN. In contrast to GaN, for which the Auger carriers occupy states near the Brillouin zone boundary,[36] the Auger electrons in InN get excited to states with small crystal momentum near Γ. Moreover, the value of the InN bandgap is smaller than the energy difference to the next conduction band (3.55 eV), and thus, only intraband processes are possible. The dependence of the direct Auger rate on the bandgap [$\propto \exp(-E_g/kT)$][37] also suggests its stronger importance in narrower-gap InN. These physical arguments are validated

by our calculations for InN (Fig. 2). The direct *eeh* Auger process is the largest contributor by a factor of 9 over the direct *hhe* process. The phonon-assisted *eeh* and *hhe* processes are both much weaker than the direct *eeh* one by approximately two orders of magnitude. Therefore, direct *eeh* Auger dominates in InN over the entire range of bandgap values we examined (0.5–0.8 eV) and should also dominate in high-In-content InGaN.

After identifying the dominant Auger process, we examine how the radiative and Auger recombination coefficients vary with carrier density (Fig. 3). At low carrier density, both recombination coefficients are constant with respect to density. But as the density increases (and the carriers become degenerate), both coefficients become decreasing functions of the density but with different characteristic density values. The radiative rate declines at a carrier density of roughly one order of magnitude smaller than the Auger rate. The efficiency of devices in this regime would suffer because of high Auger recombination but suppressed radiative recombination.

Because the Auger rate is not suppressed at the same carrier density as the radiative one, a mechanism other than phase-space filling may be responsible. To understand whether phase-space filling or screening impacts the Auger rate most, we performed calculations both with and without screening of the Coulomb interaction by free carriers. To understand the density dependence analytically, we fit our data using (Ref. 9)

$$B(n) = \frac{B_0}{1 + (n/n_0)^b}, \tag{1}$$

where $B(n)$ is the density-dependent radiative coefficient, B_0 is the coefficient in the low-density limit, n_0 is the characteristic density for the onset of phase-space filling or screening, and the exponent b is approximately equal to 1. A similar equation is used to fit the $C(n)$ coefficients. In contrast to previous work,[11,38] here, we assume the n_0 and b parameters to be different for the $B(n)$ and $C(n)$ fits. The fitted values are listed in Table I.

The radiative coefficient deviates from the non-degenerate constant value at a characteristic density $n_0 = 2.1 \times 10^{18}\,\mathrm{cm}^{-3}$,

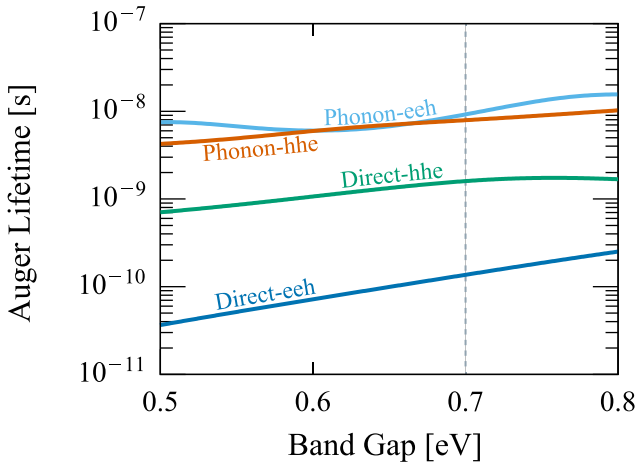

FIG. 2. Auger lifetimes of InN as a function of bandgap for the various Auger processes and for a carrier density of $10^{19}\,\mathrm{cm}^{-3}$. The rigid gap adjustment accounts for the experimental variation of the InN gap as well as simulates alloying with GaN. Direct *eeh* Auger dominates throughout the 0.5–0.8 eV gap range, as expected for narrow-gap semiconductors.

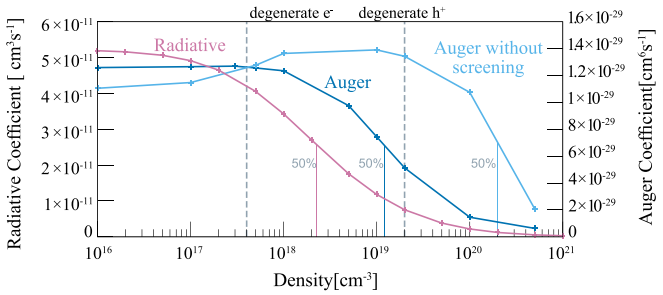

FIG. 3. Variation of the radiative and Auger (both with and without free-carrier screening) coefficients as a function of free-carrier density. The vertical dashed lines denote the densities at which carriers become degenerate, while the vertical solid lines indicate the densities at which the coefficients are reduced to 50% of their non-degenerate values. The onset of the reduction of the radiative coefficient occurs at lower carrier densities than the Auger coefficient, which is detrimental to the IQE of devices in this carrier-density range.

which is approximately one order of magnitude lower than the characteristic density of the *screened* Auger coefficient ($n_0 = 1.9 \times 10^{19}\,\mathrm{cm}^{-3}$). In comparison, the *unscreened* Auger coefficient (which is limited at high densities only by phase-space filling) has a characteristic density that is one further order of magnitude higher ($2.5 \times 10^{20}\,\mathrm{cm}^{-3}$). Meaning that the primary cause for the decline of the Auger coefficient is the screening of the Coulomb interaction, phase-space filling is a secondary effect. We note that a weaker density dependence for the C coefficient than the B coefficient has been reported in semipolar InGaN wells.[39] The unscreened Auger coefficient exhibits a small increase before the effects of phase-space filling ultimately cause the rate to decline, a behavior which is also observed in the theory work of Ref. 40 for GaSb. We expect that our conclusions on the density-dependence of the coefficients, which were derived for bulk InN, also directly apply to nonpolar quantum wells. The physics is more complex in polar and semipolar wells, in which the strong polarization fields that separate carriers and reduce the recombination rates are also screened by free carriers. However, since the polarization fields affect both the radiative and the Auger rate proportionately,[41] we expect that our conclusions about the relative importance of phase-space filling and the screening of the Coulomb interaction should also apply to the radiative and Auger coefficients of polar and semipolar wells, once their values are corrected by the overlap of the electron and hole envelope functions.

Our fits are compared to experimental Auger lifetimes in Fig. 4, which range from 20 to 1200 ps[14–17] for carrier densities in the 10^{18}–$10^{19}\,\mathrm{cm}^{-3}$ range. Our values at a carrier density of $10^{19}\,\mathrm{cm}^{-3}$ lie within this range (129 ps for unscreened Auger and 72 ps for screened Auger). Most experiments measured the Auger rate as having an n^2 dependence,[14,16,17] in agreement with our calculations. Moreover,

TABLE I. The parameters used to fit the density dependence of the radiative and Auger coefficients according to Eq. (1).

	Prefactor	n_0 (cm^{-3})	b
Auger w/ screening	$1.1 \times 10^{-28}\,\mathrm{cm}^6\,\mathrm{s}^{-1}$	1.9×10^{19}	0.98
Auger w/o screening	$1.4 \times 10^{-28}\,\mathrm{cm}^6\,\mathrm{s}^{-1}$	2.5×10^{20}	1.5
Radiative	$5.2 \times 10^{-11}\,\mathrm{cm}^3\,\mathrm{s}^{-1}$	2.1×10^{18}	0.83

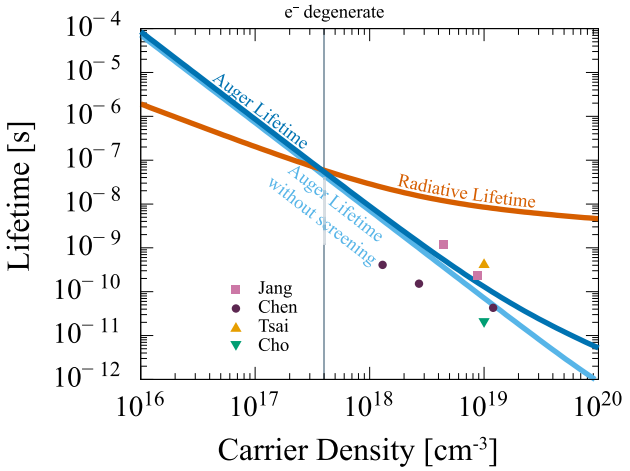

FIG. 4. Comparison of calculated Auger and radiative lifetimes with experimental values, which vary from 20 to 1200 ps in the 10^{18}–10^{19} cm^{-3} density range (Refs. 14–17). Our calculated lifetimes for both the screened and unscreened Auger processes lie within the range of experimental measurements. Auger recombination becomes stronger than the radiative process at a carrier density of 4×10^{17} cm^{-3}, at which coincidentally electrons become degenerate.

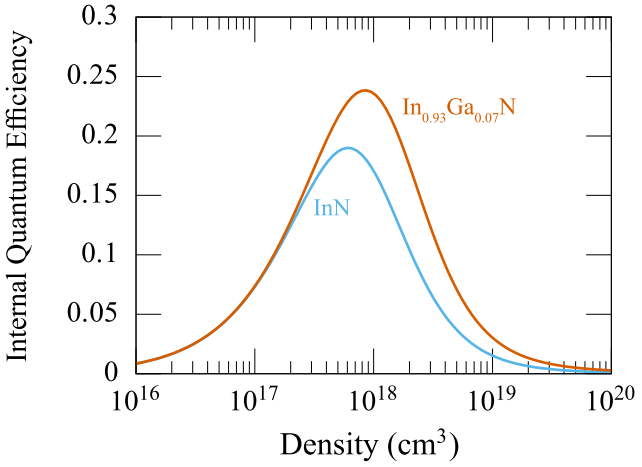

FIG. 5. Simulated internal quantum efficiency versus carrier density for InN and $In_{0.93}Ga_{0.07}N$ devices. Alloying InN with 7% GaN increases the bandgap to 0.8 eV (for light emission at 1550 nm), increases the maximum efficiency by 33%, and reduces the efficiency droop at high power.

although Chen *et al.*[17] ruled out the possibility of Auger recombination from their lifetime measurements, we find that their measured lifetimes are two orders of magnitude shorter than our calculated radiative values and are more consistent with our Auger data.

Finally, we examine how the Auger and radiative rates change when InN is alloyed with small amounts of GaN. Alloying InN with 7% GaN increases the gap to 0.8 eV and leads to emission at 1550 nm, an important optical fiber telecommunication wavelength. The Auger coefficient also decreases exponentially with the increasing bandgap. The internal quantum efficiency (IQE) is given by

$$\eta = \frac{B(n)n^2}{An + B(n)n^2 + C(n)n^3}.$$

For binary InN, we use our model Auger and radiative coefficients presented earlier, while for the $In_{0.93}Ga_{0.07}N$ alloy, we used Auger values obtained for InN with the bandgap rigidly increased to 0.8 eV. At a carrier density of 10^{18} cm^{-3}, the C coefficient decreases from 1.2×10^{-28} cm^6 s^{-1} for binary InN to 5.0×10^{-29} cm^6 s^{-1} for the $In_{0.93}Ga_{0.07}N$ alloy, i.e., a nearly 50% reduction. For A, we use an experimental value for InGaN ($A \approx 6 \times 10^7$ s^{-1}).[42] The two IQE curves are shown in Fig. 5. The IQE peak of $In_{0.93}Ga_{0.07}N$ is 33% higher than InN and occurs at a higher carrier density, which results in overall more efficient optoelectronic devices. Although we did not consider the effects of other possible energy-loss mechanisms in our analysis (e.g., carrier leakage), our results point to Auger recombination being a strong nonradiative loss mechanism in InN and In-rich InGaN optoelectronic devices and an important source of efficiency droop.

Although our analysis focused on bulk InN, our conclusions (dominant role of direct *eeh* Auger, relative importance of phase-space filling, and carrier screening) must also hold for In-rich InGaN alloys and for quantum-well structures, with best quantitative accuracy for thick nonpolar wells and for high-In-content alloys. For polar or atomically thin wells, the polarization fields and quantum confinement need to also be considered.[43] On the other hand, the effects of confinement and alloying on Auger recombination are much stronger for GaN[32,43] than for InN, since Auger in GaN is weak and only enabled by lack of momentum conservation (due to phonons, alloy disorder, confinement, etc.). For InN and In-rich InGaN, however, direct Auger is allowed and we anticipate that confinement and alloy disorder have only a minor quantitative effect on the Auger rates. Further work is needed to fully assess Auger recombination in quantum-confined InN wells and in In-rich InGaN alloys that include composition fluctuations and carrier localization.[44]

In conclusion, we found that direct *eeh* Auger is the dominant Auger process in bulk InN. Carrier degeneracy impacts Auger and radiative recombination differently. While the radiative coefficient declines because of phase-space filling, the Auger coefficient is primarily reduced by free-carrier screening at higher carrier densities. This effect suppresses the radiative rate at lower carrier densities than Auger recombination and reduces the IQE of devices. Alloying InN with GaN to increase the bandgap is an effective method to reduce the Auger rate and increase the IQE, while also shifting the emission wavelength to the 1550 nm telecommunications range.

This work was supported by the NSF (No. DMR-1254314) and the DOE NERSC Facility (No. DE-AC02-05CH11231). A.M. acknowledges support from the NSF Graduate Research Fellowship Program (No. DGE-1256260).

[1]C. J. Humphreys, MRS Bull. **33**, 459 (2008).
[2]A. Winden, M. Mikulics, A. Haab, D. Grützmacher, and H. Hardtdegen, Jpn. J. Appl. Phys. **52**, 08JF05 (2013).
[3]H. Lüth, M. Mikulics, A. Winden, S. Trellenkamp, Z. Sofer, M. Marso, D. Grützmacher, and H. Hardtdegen, in *2016 11th International Conference on Advanced Semiconductor Devices Microsystems (ASDAM)* (2016), pp. 69–72.
[4]M. M. H. Polash, M. S. Alam, and S. Biswas, Opt. Eng. **57**, 036110 (2018).
[5]J. Piprek, Phys. Status Solidi A **207**, 2217 (2010).

[6]J. Iveland, L. Martinelli, J. Peretti, J. S. Speck, and C. Weisbuch, Phys. Rev. Lett. **110**, 177406 (2013).
[7]E. Kioupakis, P. Rinke, K. T. Delaney, and C. G. Van de Walle, Appl. Phys. Lett. **98**, 161107 (2011).
[8]J. Hader, J. V. Moloney, and S. W. Koch, Appl. Phys. Lett. **87**, 201112 (2005).
[9]E. Kioupakis, Q. Yan, D. Steiauf, and C. G. Van de Walle, New J. Phys. **15**, 125006 (2013).
[10]A. David and M. J. Grundmann, Appl. Phys. Lett. **96**, 103504 (2010).
[11]A. David, N. G. Young, C. A. Hurni, and M. D. Craven, Appl. Phys. Lett. **110**, 253504 (2017).
[12]S. Okur, M. Nami, A. K. Rishinaramangalam, S. H. Oh, S. P. DenBaars, S. Liu, I. Brener, and D. F. Feezell, Opt. Express **25**, 2178 (2017).
[13]T. H. Ngo, B. Gil, B. Damilano, P. Valvin, A. Courville, and P. de Mierry, J. Appl. Phys. **122**, 063103 (2017).
[14]T.-R. Tsai, C.-F. Chang, and S. Gwo, Appl. Phys. Lett. **90**, 252111 (2007).
[15]D.-J. Jang, G.-T. Lin, C.-L. Hsiao, L. Tu, and M.-E. Lee, Appl. Phys. Lett. **92**, 042101 (2008).
[16]Y. Cho, X. Lue, M. Wienold, M. Ramsteiner, H. T. Grahn, and O. Brandt, Phys. Rev. B **87**, 155203 (2013).
[17]F. Chen, A. Cartwright, H. Lu, and W. Schaff, Phys. Status Solidi A **202**, 768 (2005).
[18]K. Delaney, P. Rinke, and C. G. Van de Walle, Appl. Phys. Lett. **94**, 191109 (2009).
[19]P. Giannozzi, S. Baroni, N. Bonini, M. Calandra, R. Car, C. Cavazzoni, D. Ceresoli, G. L. Chiarotti, M. Cococcioni, I. Dabo, A. Dal Corso, S. de Gironcoli, S. Fabris, G. Fratesi, R. Gebauer, U. Gerstmann, C. Gougoussis, A. Kokalj, M. Lazzeri, L. Martin-Samos, N. Marzari, F. Mauri, R. Mazzarello, S. Paolini, A. Pasquarello, L. Paulatto, C. Sbraccia, S. Scandolo, G. Sclauzero, A. P. Seitsonen, A. Smogunov, P. Umari, and R. M. Wentzcovitch, J. Phys.: Condens. Matter **21**, 395502 (2009).
[20]J. P. Perdew and A. Zunger, Phys. Rev. B **23**, 5048 (1981).
[21]A. Terentjevs, A. Catellani, D. Prendergast, and G. Cicero, Phys. Rev. B **82**, 165307 (2010).
[22]D. Bayerl and E. Kioupakis, Nano Lett. **14**, 3709 (2014).
[23]J. Deslippe, G. Samsonidze, D. A. Strubbe, M. Jain, M. L. Cohen, and S. G. Louie, Comput. Phys. Commun. **183**, 1269 (2012).
[24]V. Davydov, A. Klochikhin, R. Seisyan, V. Emtsev, S. Ivanov, F. Bechstedt, J. Furthmüller, H. Harima, A. Mudryi, J. Aderhold, O. Semchinova, and J. Graul, Phys. Status Solidi B **229**, r1 (2002).
[25]J. Wu, W. Walukiewicz, K. Yu, J. Ager Iii, E. Haller, H. Lu, W. J. Schaff, Y. Saito, and Y. Nanishi, Appl. Phys. Lett. **80**, 3967 (2002).
[26]C. S. Gallinat, G. Koblmüller, J. S. Brown, S. Bernardis, J. S. Speck, G. D. Chern, E. D. Readinger, H. Shen, and M. Wraback, Appl. Phys. Lett. **89**, 032109 (2006).
[27]P. D. C. King, T. D. Veal, C. E. Kendrick, L. R. Bailey, S. M. Durbin, and C. F. McConville, Phys. Rev. B **78**, 033308 (2008).
[28]J. Wu, W. Walukiewicz, W. Shan, K. M. Yu, J. W. Ager, E. E. Haller, H. Lu, and W. J. Schaff, Phys. Rev. B **66**, 201403 (2002).
[29]N. Marzari, A. A. Mostofi, J. R. Yates, I. Souza, and D. Vanderbilt, Rev. Mod. Phys. **84**, 1419 (2012).
[30]A. A. Mostofi, J. R. Yates, Y.-S. Lee, I. Souza, D. Vanderbilt, and N. Marzari, Comput. Phys. Commun. **178**, 685 (2008).
[31]B. K. Ridley, *Quantum Processes in Semiconductors* (Clarendon Press, Oxford, 1982).
[32]E. Kioupakis, D. Steiauf, P. Rinke, K. T. Delaney, and C. G. Van de Walle, Phys. Rev. B **92**, 035207 (2015).
[33]G. Cappellini, R. Del Sole, L. Reining, and F. Bechstedt, Phys. Rev. B **47**, 9892 (1993).
[34]V. W. L. Chin, T. L. Tansley, and T. Osotchan, J. Appl. Phys. **75**, 7365 (1994).
[35]K. A. Bulashevich and S. Y. Karpov, Phys. Status Solidi C **5**, 2066 (2008).
[36]E. Kioupakis, P. Rinke, A. Schleife, F. Bechstedt, and C. G. Van de Walle, Phys. Rev. B **81**, 241201 (2010).
[37]A. R. Beattie and P. T. Landsberg, Proc. R. Soc. London A **249**, 16–29 (1959).
[38]A. David and N. F. Gardner, Appl. Phys. Lett. **97**, 193508 (2010).
[39]M. Monavarian, A. Rashidi, A. A. Aragon, S. H. Oh, M. Nami, S. P. DenBaars, and D. F. Feezell, Opt. Express **25**, 19343 (2017).
[40]A. Haug, J. Phys. C: Solid State Phys. **16**, 4159 (1983).
[41]E. Kioupakis, Q. Yan, and C. G. Van de Walle, Appl. Phys. Lett. **101**, 231107 (2012).
[42]Y. Shen, G. Mueller, S. Watanabe, N. Gardner, A. Munkholm, and M. Krames, Appl. Phys. Lett. **91**, 141101 (2007).
[43]F. Bertazzi, X. Zhou, M. Goano, G. Ghione, and E. Bellotti, Appl. Phys. Lett. **103**, 081106 (2013).
[44]C. M. Jones, C. H. Teng, Q. Yan, P. C. Ku, and E. Kioupakis, Appl. Phys. Lett. **111**, 113501 (2017).